Generation of low-energy neutral beam for Si etching

S. J. Kim, S. J. Wang, and J. K. Lee[a)]
Department of Electronic and Electrical Engineering, Pohang University of Science and Technology, Pohang 790-784, South Korea

D. H. Lee and G. Y. Yeom
Department of Materials Engineering, Sungkyunkwan University, Suwon 440-746, South Korea

(Received 29 August 2003; accepted 24 May 2004; published 20 September 2004)

As the feature size shrinks toward the nanoscale, charge-up damage from ion-induced etching becomes a very serious problem. Neutral beam etching is one of the most popular techniques used to reduce charge-up damage. We have performed a neutral beam simulation to optimize the neutral beam, which is generated by collisions between ions produced by a plasma source with an ion gun and low angle reflectors. An ion gun is simulated using the two-dimensional Xgrafic object oriented particle-in-cell (XOOPIC) code to obtain a higher ion flux and to improve the directionality of ions. For neutral beam simulation, we use the modified XOOPIC code to which reflection data obtained by the transport of ions in matter (TRIM) code are appended. Neutral flux, energy and angle distributions, which have an influence upon the etch rate, are calculated in the neutral beam simulation. A low-energy neutral beam from an ion gun with two grids has a low neutral flux and a broad angle distribution. Therefore, we propose a three-grid ion gun that has one additional grid with positive voltage, allowing independent control of the ion flux and ion energy. By increasing the ion flux, the neutral flux by three grids is three times larger than that by two grids. The neutral beam source using a three-grid ion gun has several advantages for trench etching: increased etch rate, decreased sidewall etching, and reduced variation in the etch rate as the trench size changes. A low-energy neutral beam source using the three-grid ion g 0un and low-angle reflectors is experimentally tested. © *2004 American Vacuum Society.* [DOI: 10.1116/1.1774198]

I. INTRODUCTION

The characteristics of the etching process, such as the etch rate, selectivity, uniformity, directionality, surface quality and reproducibility, have been intensively studied. Despite steady progress in the field, plasma process induced damage (PPID), which affects device reliability, is an inevitable problem. Reactive ion etching, where energetic charged particles which activate a reactive etchant and induce anisotropic etching, has significant problems because the motion of ions and electrons projected at the wafer are different because, while ions have anisotropic motion, electrons have isotropic motion. The difference in accumulated charge generates a potential difference in the shallow trench,[1] causing charge-up damage such as the electron shading effect, notching, and early etch stop.[2–4] It also has a harmful effect on the reliability of the thin oxide layer because of charge trapping.[5] As the feature size shrinks, these problems become more important. Neutral beam etching[6–9] has thus been proposed as a means by which to eliminate charge-up damage. Important issues in neutral beam etching are the methods of generating the ion source and the neutral beam and controlling the neutral beam energy and angle. Various neutral beam sources have been studied for neutral beam etching.

We have studied neutral beam generation using an ion gun and low-angle reflectors.[10,11] A schematic of our two-grid neutral beam source is shown in Fig. 1. Plasma is created by an inductively coupled plasma (ICP) source. Only positive ions pass through the hole in the grids. They are accelerated toward the low-angle reflectors and neutralized by collisions with reflectors. In this neutral beam source, voltages applied to the grid control the neutral energy. In our study, we have performed a neutral beam generation simulation using the xgraphic object oriented particle-in-cell (XOOPIC) code, which is a well-known two-dimensional particle-in-cell code that calculates characteristics of plasma.[12] The ion flux, energy, and angle distributions are optimized by varying the hole size, grid gap, and grid voltage in the ion gun. Ion characteristics have an influence on the reflection coefficient and angle. The influence of reflection conditions (reflector length, material, pressure, and others) on the properties of the neutral beam were investigated, and provided estimates of the neutral flux, energy, and angle distribution necessary for realizing high performance neutral etching.

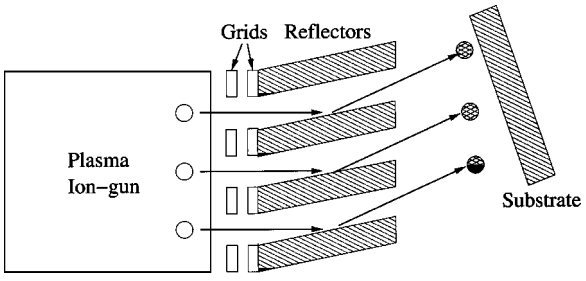

FIG. 1. Schematic of the configuration of the neutral beam source.

a)Electronic mail: jkl@postech.ac.kr

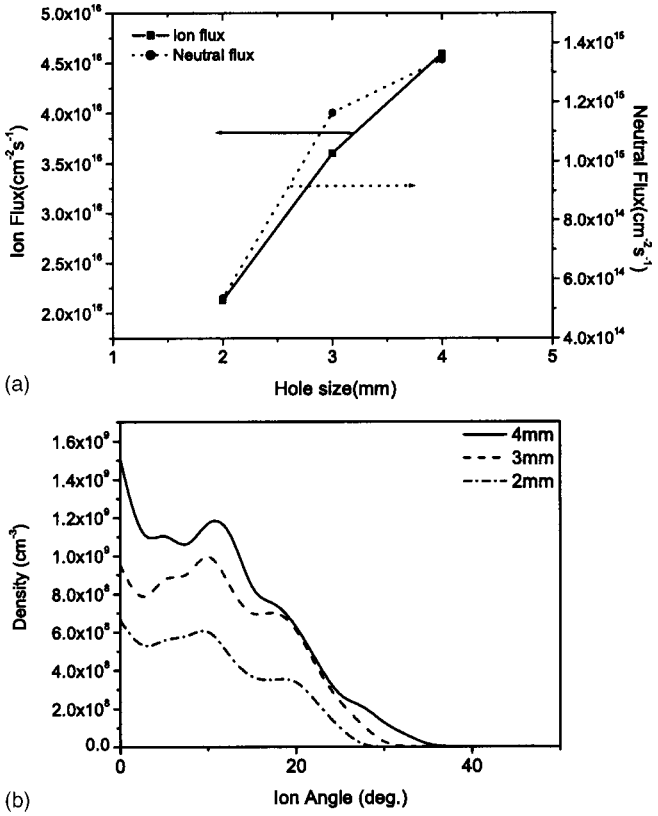

FIG. 2. Characteristics of the ion gun for various hole sizes. (a) Ion and neutral fluxes and (b) ion angle distribution.

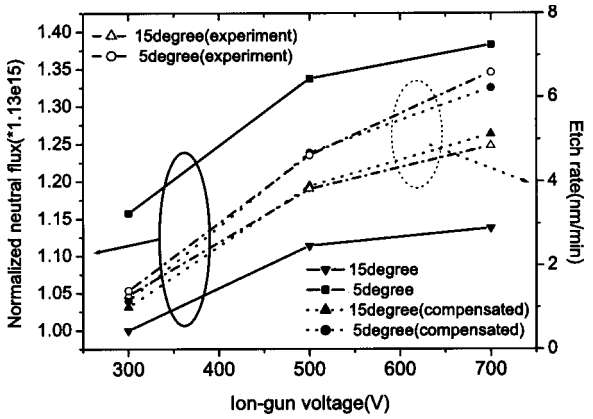

FIG. 3. Neutral flux (solid lines) and etch rate (dotted lines) in the simulation and PR etch rate (dotted-dashed lines) from O_2 gas in the experiment vs the ion gun voltage for different reflector angles.

The activation energy barrier for chemical reaction is below 1–2 eV,[13] but impingement energies of more than 20 eV cause nuclear displacement damage.[14] Low-energy neutrals below 20 eV are required for Si etching in which chemical reactions are dominant.[15,16] A three-grid ion gun is proposed in order to obtain high flux and low-energy neutrals. Compared with a two-grid ion gun, the three-grid ion gun has advantages for the etching process. We have exam-

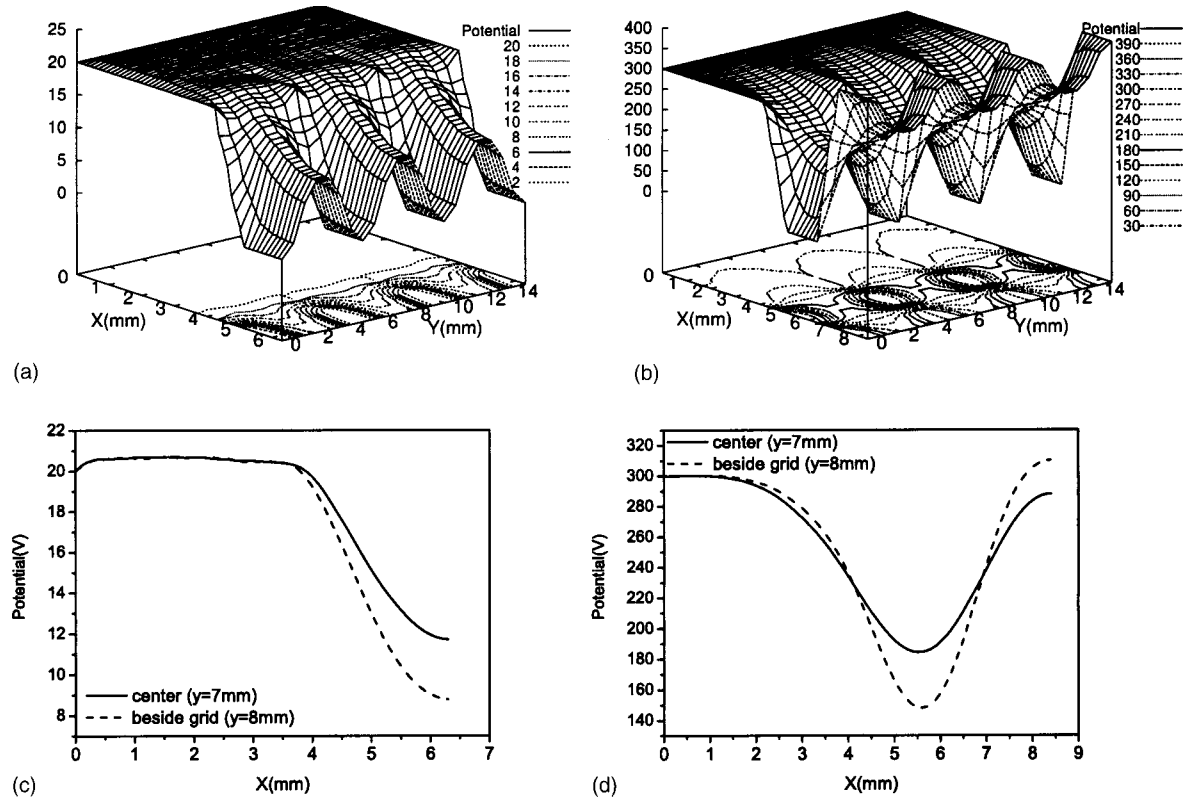

FIG. 4. Potential generated by being applied grid voltages. Potential contours in (a) two-grid ion gun and (b) three-grid ion gun. Potential profile for $y=7$ and 8 mm in (c) two-grid ion gun and (d) three-grid ion gun. The solid line is potential in the center ($y=7$ mm) of the hole, and the dashed line is potential in the middle ($y=8$ mm) between the grid and the center of the hole.

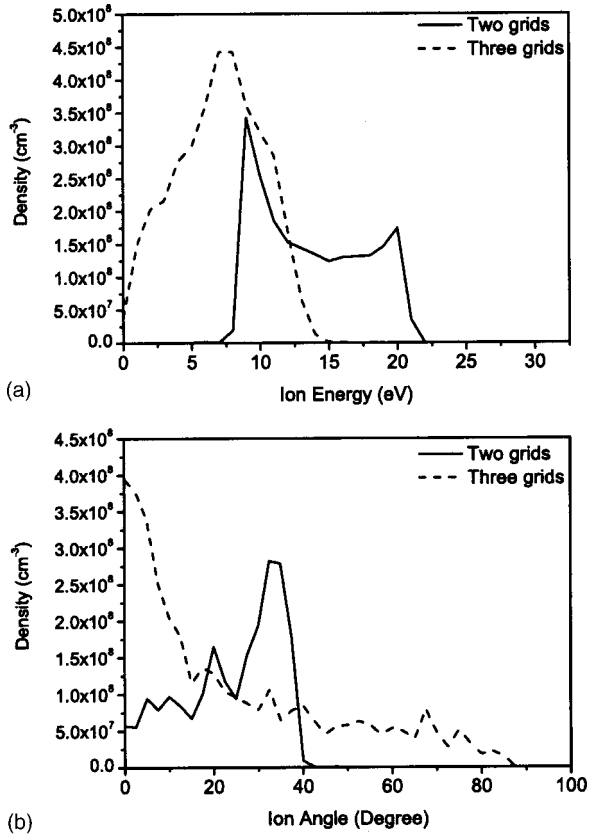

FIG. 5. (a) Ion energy distribution and (b) ion angle distribution in two-grid and three-grid ion guns.

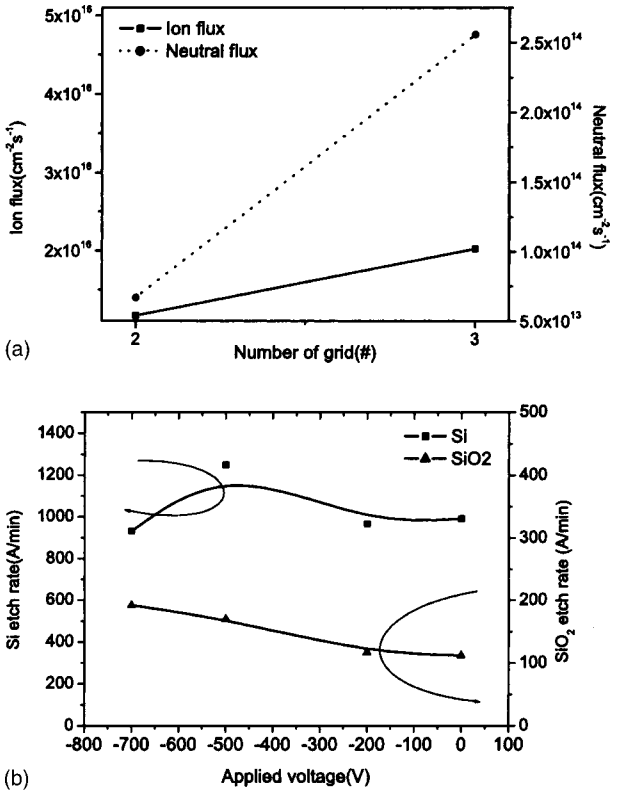

FIG. 6. (a) Simulation results of ion flux and neutral flux for low-energy particles and (b) experimental results for Si and SiO_2 etch rates from the three-grid ion gun. Experimental conditions: $V_1=400$ V, $V_2=0$ V, $V_3=-400-400$ V, pure SF_6, gas flow rate=20 sccm. The voltage applied is V_3-V_1.

ined the ion flux, the energy, and the angle distribution generated by the three-grid ion gun. Its effects are verified in an experiment on Si etching.

II. SIMULATION OF NEUTRAL BEAM GENERATION

The neutral beam generation simulation is comprised of the ion gun simulation and the neutral beam simulation. The ion gun simulation is conducted separately from the neutral beam simulation because of the difference in mesh size of the simulation. Although the energy and the angle of ions depend on ion gun parameters such as the grid voltage, grid width, grid interval, and hole size, they are difficult to predict. The ion energy and the angle distributions are calculated from the XOOPIC code, which appropriately represents energy and angle distributions of ions and electrons, in order to optimize the ion beam source. Ion flux from the ion gun must be high with low angle distributions. The ion gun is composed of two grids controlled by an external voltage source. To accelerate positive ions, positive voltage is applied to the first grid and negative or 0 V is applied to the second grid. Only positive ions are ejected by the electric field between the two grids. If electrons are present in the etcher, ultraviolet (UV) radiation from excited states produced by inelastic collisions between neutrals and electrons causes damage in the neutral etching process.[17,18] For this reason, it is necessary to eliminate electrons from the process. The grid thickness and the gap between grids, which are related to ion loss and the electric field, are important parameters that determine the performance of the ion gun.

The ion energy and the angle calculated by the ion gun simulation are the input parameters for the neutral beam generation simulation. As ions approach a high-work function metal, they are neutralized through a resonant neutralization process and an Auger capture process. Since the phenomenon of collisions between ions and reflectors is very complicated and there is a lack of theory and experimental data for ions with energies of hundreds of eV, it is difficult to determine the rate of reflection and neutralization. Therefore, we have considered a computational model using the Monte Carlo method of random sampling known as transport of ions in matter (TRIM).[19,20] Characteristics such as the reflection coefficient, energy and angle distributions of reflected particles calculated by the TRIM code are appended to the XOOPIC code. In general, the flux and the energy of reflected particles have been calculated as follows:[21]

$$R_N(E_{\text{in}},\theta)=1.0+\left(1.0-\frac{\theta}{90^\circ}\right)[R_N^\circ(E_{\text{in}})-1.0], \tag{1}$$

$$R_E(E_{\text{in}},\theta)=1.0+\left(1.0-\frac{\theta}{90^\circ}\right)[R_E^\circ(E_{\text{in}})-1.0], \tag{2}$$

where

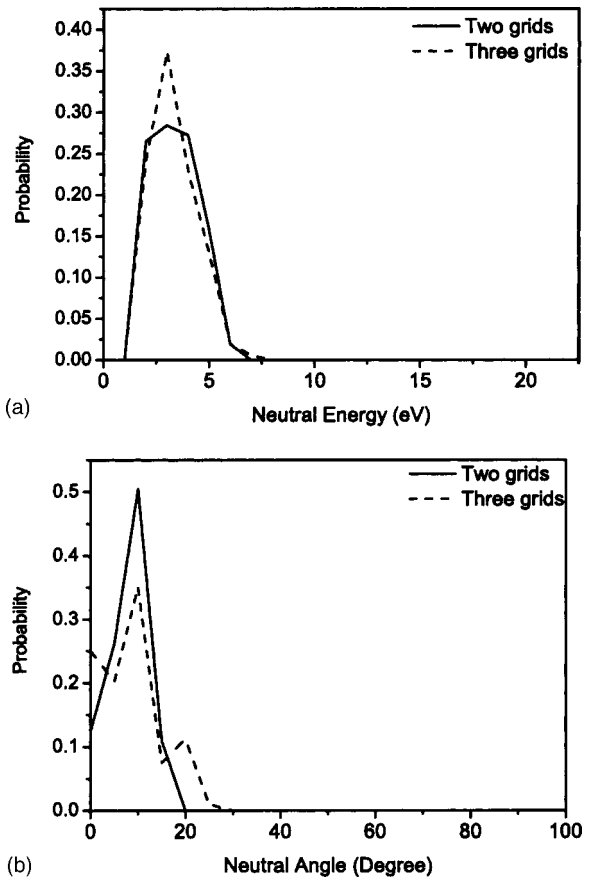

FIG. 7. (a) Neutral energy distribution and (b) neutral angle distribution by two-grid and three-grid ion guns.

$$R_N^{\circ}(E_{\text{in}}) = -0.237 \log(E_{\text{in}}/E_L) + 0.19,$$

$$R_E^{\circ}(E_{\text{in}}) = -0.220 \log(E_{\text{in}}/E_L) + 0.06.$$

R_N and R_E are reflection coefficients of the neutrals and energies as a function of the incident energy and angle. θ is the normal incident angle. E_L is the energy reduction constant with respect to reflector materials in order to obtain reduced energy of incident ions and E_{in} is the incident energy. The energy of reflected particles is proportional to R_E, which depends on the incident ion energy and normal incident ion angle. The angular distribution of reflected particles is calculated from[21]

$$\phi = \arctan\left\{\sin\theta \Big/ \left[\cos\theta + \left(\frac{M_1}{M_2}\right)\right]\right\}, \tag{3}$$

where M_1/M_2 is the mass ratio between the incident ions and the reflector. Reflection is dependent on the incident energy and angle. The reflected angle distribution has a cosine distribution based on the incident ion angle. The quantity of reflected neutrals increases at high normal incident angles. It can be assumed that most of the reflected particles are neutrals based on Hagstrum's model and on work by Graves and co-workers.[22,23] Thus, the neutral beam is optimized by varing the reflection conditions in order to obtain a high neutral flux, which is related to the etch rate, and easily controllable neutral energy. In this simulation, Ar gas is used to obtain fundamental characteristics of the reflected neutral beam.

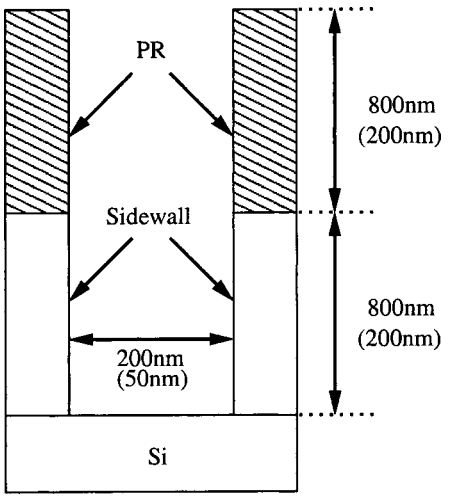

FIG. 8. Schematic of simulated domain of the shallow trench structure. The trench width is 200 or 50 nm. The aspect ratio is 8. The sidewall of the trench is composed of photoresist and silicon layers.

III. SIMULATION RESULTS

A. Neutral beam generation

The grid width of the ion gun used in the simulation is 1.2 mm, and the interval between the grids is 0.9 mm. A low pressure of 0.1 mTorr is used in order to obtain a narrow ion angle distribution. The ion flux and the angle distribution are shown in Fig. 2 as a function of the hole size. As the hole size increases from 2 to 4 mm, the ion flux increases linearly, but the ion angle distribution becomes broader because ions can enter the hole more easily. This large ion angle distribution, one of the important factors controlling neutral flux, results in a relatively smaller change in neutral flux. Grid voltages of the ion gun control ion and neutral fluxes. The neutral flux versus grid voltage and reflector angle (solid lines) is shown in Fig. 3. A higher ion gun voltage and lower-angle reflector create a higher neutral flux because the high energy and the large incident ion angle give a large reflection coefficient. The etch rate (ER) can be assumed to be proportional to the neutral flux. The etch rate is described as follows:

$$\text{etch rate} = \alpha \times \Gamma_n, \quad \alpha = a \times \beta(E,\theta), \tag{4}$$

where a is the constant of proportionality, $\beta(E,\theta)$ is the etch rate function, which is related with the energy and normal incident angle of particles and Γ_n is the neutral flux. The experimental results of the photoresist (PR) etch rate versus the grid voltage and the reflector angle (dotted-dashed lines) are shown in Fig. 3. By comparing the results for a system with a 15° reflector angle in the simulation (marked by inverted triangles) with the same angle in the experiment (marked by open triangles), a calibration factor (α) is calculated. In this case, α is approximately $3.5/1.13\times10^{-15}$ and $4.5/1.13\times10^{-15}$ cm^{-2} s^{-1} for 500 and 700 V ion guns, re-

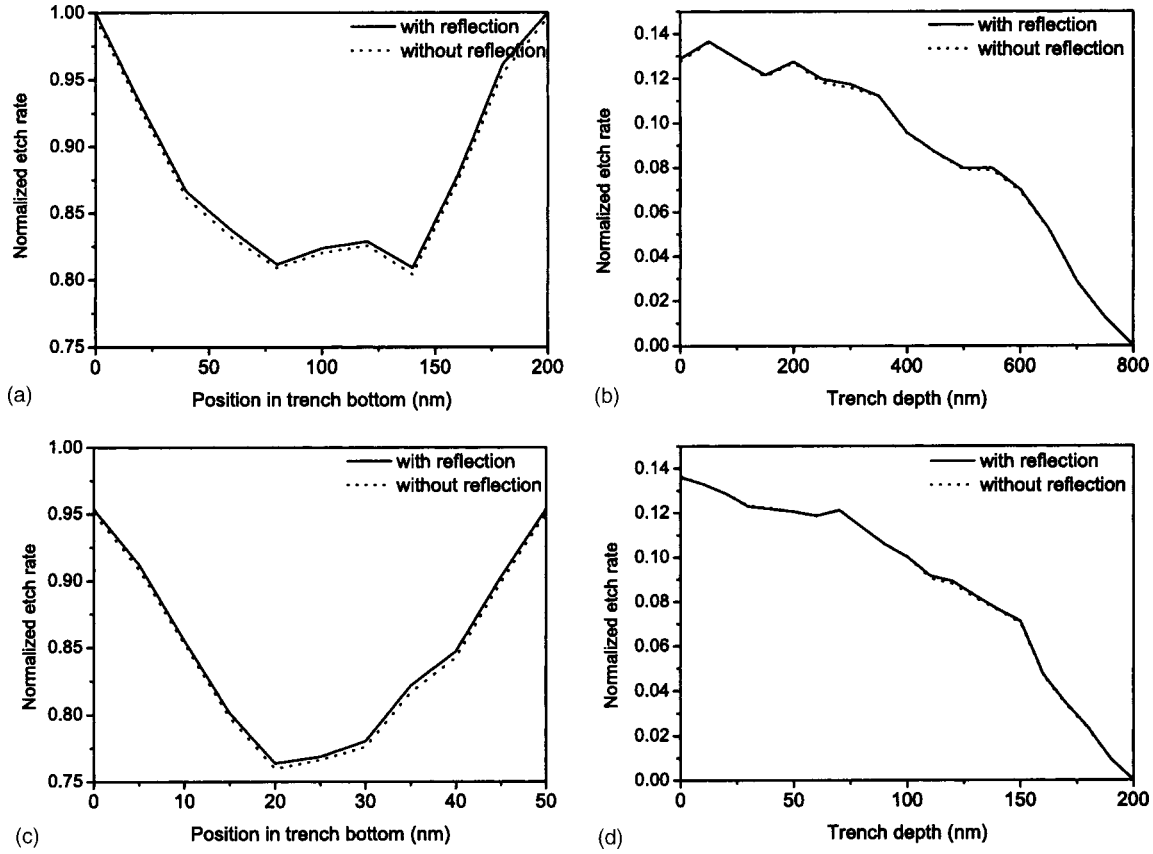

FIG. 9. Normalized etch rate along the wall of the structure using two grids: (a) at the bottom of the 200 nm trench, (b) at the sidewall of the 200 nm trench, (c) at the bottom of the 50 nm trench, and (d) at the sidewall of the 50 nm trench. The normalized etch rate is calculated on the basis of a maximum vertical etch rate of a 200 nm trench.

spectively. These values can be used to convert the data for the 5° simulation (marked by rectangles) to etch rates. The simulation results are in agreement with the experimental results for a reflector angle of 5°. The low-angle reflector and the high grid voltage result in a high etch rate, as shown in Fig. 3. Generally, the etch rate is proportional to the neutral flux and neutral energy. The reflection efficiency of ions increases at low collision angles between ions and the reflectors. Thus, a low-angle reflector results in high neutral flux and a high etch rate. The directionality of ions is also important in order to maintain low-angle collisions. All these factors are important for the improvement of neutral beam sources.

B. Low-energy neutral beam for Si etching

A neutral beam more energetic than 100 eV is too high for Si etching.[16] Low-energy neutrals (10–20 eV) are required to reduce physical and charge-up damage. In the two-grid ion gun, low energy neutrals can be obtained by decreasing the grid voltage. However, the ion flux, and thus the neutral flux, also decreases with it. The first grid voltage determines the sheath structure around the hole,[24] which is closely connected with the ion flux and angle distribution. Therefore, a three-grid ion gun is proposed to obtain high flux and low energy neutrals. The three-grid ion gun has an additional positive voltage grid. In order to obtain a neutral beam with energy less than 20 eV, 300, 0, and 390 V are applied to the grids. The ion flux depends on the difference in potential between the first grid (300 V) and the second grid (0 V). This difference between the first grid and the third grid (390 V) has an influence upon the ion energy. In the two-grid ion gun, the ion flux and the ion energy cannot be controlled separately. However, the three-grid ion gun allows independent control of both, preventing reduction of ion flux for low-energy ions. Potential profiles of the two-grid and the three-grid ion guns are shown in Figs. 4(a) and 4(b). These ion guns in the simulation have three 4 mm holes. In Figs. 4(a) and 4(b), hole regions are $y=0-4$ mm, $y=5-9$ mm, and $y=10-14$ mm. A potential of 20 V is applied to the first grid in the two-grid ion gun in order to obtain a low-energy ion source. The relation between the voltages of the two grids determines the potential inside the hole. Potential profiles in the center ($y=7$ mm) of the hole and in the middle ($y=8$ mm) between the grid and the center of the hole are shown in Figs. 4(c) and 4(d). The two-grid ion gun has only one acceleration region, which controls both the ion flux and the ion energy. The three-grid ion gun has both an acceleration region and a deceleration region that control the ion energy. The positive voltage of the third grid also prevents ions from dispersing toward the grids. This improves the

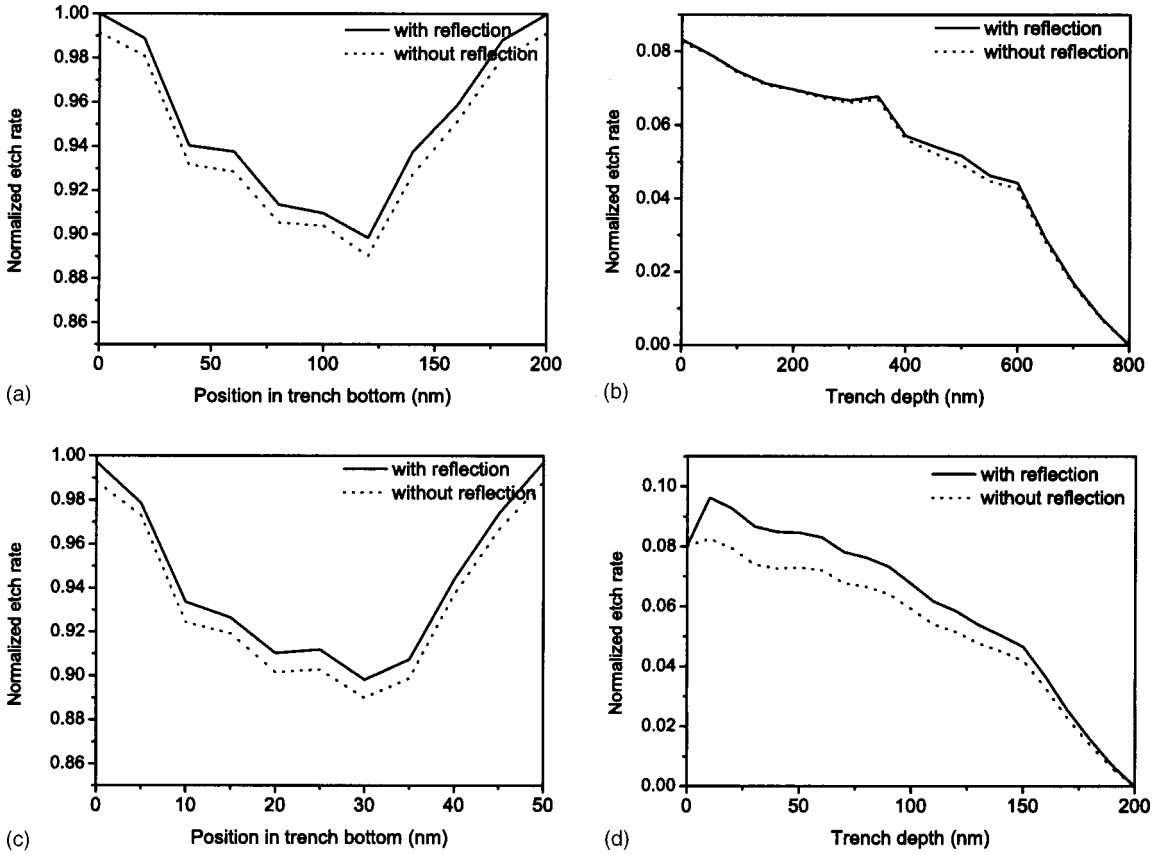

FIG. 10. Normalized etch rate along the wall of the structure using three grids: (a) at the bottom of 200 nm trench, (b) at the sidewall of the 200 nm trench, (c) at the bottom of the 50 nm trench, and (d) at the sidewall of the 50 nm trench. The normalized etch rate is calculated on the basis of a maximum vertical etch rate of a 200 nm trench.

directionality of ions, making it easy to control the incident ion angle. While the ion energy in the center of the hole is smaller than that near the grids in the two-grid ion gun, the ion energy in the three-grid ion gun is largest in the center of the hole. It concentrates ions in the center of the hole, thus improving reflection characteristics. Ion energy and angle distribution in the two-grid and three-grid ion guns are shown in Fig. 5. The dominant ion energy in Fig. 5 is nearly the same as the difference in potential in the center ($y = 7$ mm) of the hole, as shown in Figs. 4(c) and 4(d). In Figs. 4(a) and 4(b), while the two-grid ion gun has the largest difference in potential near grids, the three-grid ion gun has the largest difference in the center of hole. Maximum and minimum ion energies are also near the grid and in the center of the hole in the two-grid ion gun. The distribution of the potential of the three-grid ion gun is opposite that of the two-grid ion gun. The ion energy distribution is closely connected to the potential inside the hole. The directionality of ions in the three-grid ion gun is superior to that using the two-grid one because the positive voltage of the third grid prevents ion dispersion. Since the reflection efficiency of ions increases at low collision angles between ions and reflectors, the directional rate of ions, which is the ratio of ions having 0° directionality over the total number of ions, is more important than the tail for angles greater than 80°. Thus, the three-grid ion gun has easily controllable low-energy ions with improved directionality.

The ion and neutral fluxes in the two-grid and three-grid ion guns are shown in Fig. 6(a). The increase of ion flux results from the acceleration potential between the first grid and the second grid in the three-grid ion gun. Although the ion flux in the three-grid ion gun is about two times greater than in the two-grid one, the neutral flux increases by about a factor of 3, because ions with better directionality are focused on the center of the hole. The effect of the three-grid ion gun is verified experimentally [see Fig. 6(b)]. In the experiment, the first and second grid voltages are 400 and 0 V, respectively. The third gird voltage is varied from −400 to 400 V. The voltage applied [x axis, in Fig. 6(b)] is the difference in voltage ($V_3 - V_1$) between the first grid and the third grid. The neutral energy is approximately half the applied voltage in our neutral beam source. When the applied voltage of the third grid is increased, the SiO_2 etch rate decreases but the Si etch rate is nearly constant. Generally, the Si etch rate is controlled by the neutral flux, and the SiO_2 etch rate is influenced by neutral flux and the energy. Thus, it is verified that the ion energy rather than the ion flux is reduced in the three-grid ion gun. High flux and low-energy

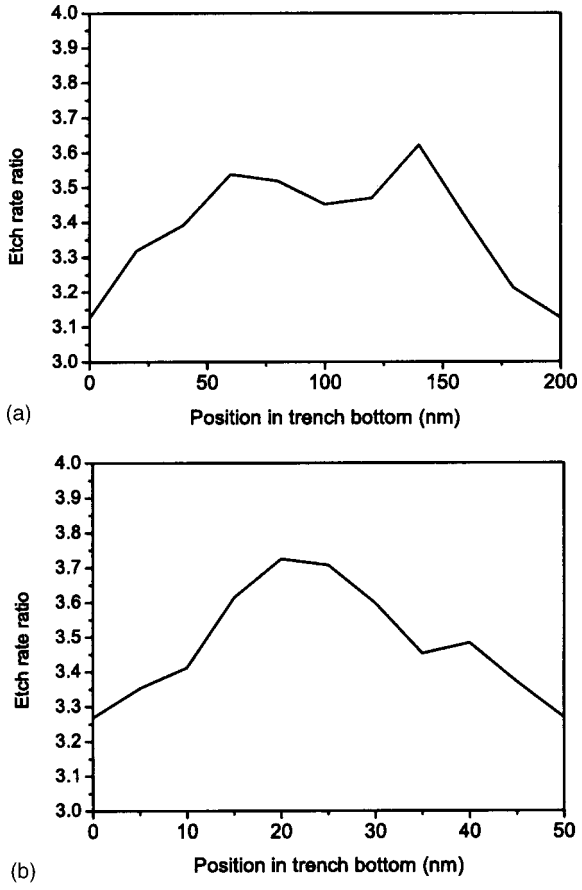

FIG. 11. Comparisons of etch rates between the two-grid and the three-grid ion guns: (a) 200 nm trench and (b) 50 nm trench. The etch rate ratio is defined as the etch rate of the three-grid ion gun to the etch rate of the two-grid ion gun.

neutrals are obtained from the three-grid ion gun. The etch rate is higher than that with the two-grid ion gun due to higher neutral flux.

The neutral energy and the angle distribution from 5° and 46 mm multireflectors using the two-grid and the three-grid ion gun are shown in Fig. 7. The use of the low-angle reflectors with a large reflection coefficient causes high neutral flux. The reflector length is determined by considering the hole size and the incident ion angle. An appropriate reflector length reduces ions which undergo no collision with reflectors and also the secondary collisions of neutrals. Although the neutral energy distributions by both the two grids and the three grids are the same, the directionality of neutrals for the three-grid ion gun is better than that for the two-grid ion gun with the same reflector. Since a longer reflector can remove high angle neutrals due to reflector blocking, the directional rate of neutrals, which is the ratio of neutrals having 0° directionality over the total number of neutrals, is more important than the broader distribution and tail for angles greater than 80°.

In order to observe the etch profile and evaluate etch characteristics of the neutral beam generated by the three-grid ion gun, we performed a shallow trench etching simulation. The shallow trench structures, in which the trench width is 200 or 50 nm, are schematically shown in Fig. 8. The aspect ratio (AR) of the shallow trench structures is 8. The sidewall is composed of PR and silicon layers four times the trench width. Since the Si etch rate is proportional to the neutral flux in the case of gas species like SF_6, the relative etch rate according to the trench position was calculated using the neutral flux, the energy and the angle distribution obtained by the neutral beam simulation. The sidewall etch rate was calculated as a function of time by considering a neutral flux rate, because the quantity of neutrals striking the sidewall changes with the time and trench depth. This included sidewall reflections from the collision between neutrals and PR or Si. The dissociation and the diffusion of neutrals into the trench were neglected, and the sidewall protection layer was not taken into consideration.

The normalized etch rates for 200 and 50 nm trenches obtained using the two-grid ion gun are shown in Fig. 9. The normalized etch rate is relative to the maximum vertical etch rate at the position of 200 nm trench bottom. The normalized etch rate of the 50 nm trench, calculated on the basis of a maximum etch rate of 200 nm, is presented in Fig. 9(c). Sidewall etch rates normalized for the vertical etch rate are shown in Figs. 9(b) and 9(d). Since higher-angle neutrals are shaded by the sidewall of the narrower trench, the etch rate for 200 nm is larger than for 50 nm. The gradient of the etch rate appears at the bottom of the trench due to high-angle neutrals (more than 5°). Although the etch rate decreases with an increase of reflector length, the gradient of the etch rate at the bottom of the trench is reduced by the corresponding elimination of high-angle neutrals. Normalized etch rates by the three-grid ion gun are shown in Fig. 10. Compared with the two-grid ion gun, the three-grid ion gun has a more uniform etch rate at the bottom of the trench and less sidewall etching. It also has closer etch rates for the 200 and 50 nm trenches than the two-grid one. There is less sidewall etching with the three-grid ion gun due to the smaller angular distribution of neutrals. The sidewall etch rate decreases with increases in etch depth for both ion guns.

The vertical etch rate using the three-grid ion gun is compared with one using the two-grid ion gun (see Fig. 11). The etch rate ratio is defined as the etch rate of the three-grid ion gun to the etch rate of the two-grid ion gun in Fig. 11. The three-grid etch rate is about three times larger than the other because of higher neutral flux and better directionality of neutrals. Also, the difference in etch rate across the bottom of the trench and between trenches of different width is less for three-grid ion gun due to higher-angle directionality of neutrals.

IV. CONCLUSIONS

An ion beam produced by a plasma source equipped with an ion gun and low-angle reflectors were used to generate a neutral beam. We performed a neutral beam generation simulation to optimize the neutral beam source, and produced high neutral flux to increase the etch rate. The neutral flux, the energy and the angle distributions were calculated. The efficiency of neutral generation depends on the ion flux, in-

cident ion energy and angle, and thus on ion gun parameters such as the grid voltage, the hole size, the grid width, and the pressure. As the hole size increases, the ion flux increases, but the ion angle becomes broader. Therefore, the rate of change of the neutral flux is smaller than that of the ion flux because of the smaller reflection from the large incident angle. As shown in both simulation and experiment, a lower-angle reflector and an increase of grid voltage lead to an increase in the PR etch rate since the etch rate is dependent on the neutral flux, energy, and angle.

For Si etching, a low-energy neutral beam is obtained by the three-grid ion gun. The potential between the first and the second grid determines the ion flux, and the third grid controls the ion energy. Thus, the three-grid ion gun allows independent control of the ion flux and the ion energy. The three-grid ion gun has three times the ion flux of a two-grid ion gun which has the same ion energy. Because of its higher neutral flux, the etch rate of the three-grid ion gun is also higher. Since the ion angle becomes more directional due to the third positive grid voltage, the directionality of neutrals increases. A neutral beam source using a three-grid ion gun has several advantages in trench etching: an increased etch rate, decreased sidewall etching, and few changes in the etch rate as the trench size changes. Therefore, it is an applicable neutral beam source for charge-up free, nanoscale Si etching. Our simulation using the XOOPIC code is useful for designing and optimizing a three-grid ion gun.

ACKNOWLEDGMENTS

The authors would like to thank Professor D. B. Graves, Dr. M. S. Hur, and Dr. H. J. Lee, for their advice and discussions. This work was supported in part by the Tera-level Nano Devices Project, 21 *c* Frontier R&D Program of the Korea Ministry of Science and Technology.

[1]G. S. Hwang and K. P. Giapis, Appl. Phys. Lett. **71**, 458 (1997).
[2]T. Kinoshita, M. Hane, and J. P. McVittie, J. Vac. Sci. Technol. B **14**, 560 (1996).
[3]J. Matsui, N. Nakano, Z. L. Petrovic, and T. Makabe, Appl. Phys. Lett. **78**, 883 (2001).
[4]G. S. Hwang, and K. P. Giapis, Appl. Phys. Lett. **74**, 932 (1999).
[5]K. Hashimoto, Jpn. J. Appl. Phys., Part 1 **33**, 6013 (1994).
[6]H. Kinoshita, M. Umeno, M. Tagawa, and N. Ohmae, Surf. Sci. **440**, 49 (1999).
[7]K. P. Giapis, T. A. Moore, and T. K. Minton, J. Vac. Sci. Technol. A **13**, 959 (1995).
[8]S. R. Leone, J. Appl. Phys. **34**, 2073 (1995).
[9]M. J. Gechner, T. K. Bennett, and S. A. Cohen, Appl. Phys. Lett. **71**, 980 (1997).
[10]D. H. Lee, J. W. Bae, S. D. Park, and G. Y. Yeom, Thin Solid Films **389–399**, 647 (2001).
[11]M. S. Hur, S. J. Kim, H. S. Lee, J. K. Lee, and G. Y. Yeom, IEEE Trans. Plasma Sci. **30**, 110 (2002).
[12]J. P. Verboncoeur, A. B. Langdon, and N. T. Gladd, Comput. Phys. Commun. **87**, 199 (1995).
[13]Stephen R. Leone, Jpn. J. Appl. Phys., Part 1 **34**, 2073 (1995).
[14]R. Behrisch, G. Maderlechner, B. M.U. Scherzer, and M. T. Robinson, J. Appl. Phys. **18**, 391 (1979).
[15]C. A. Nichols and D. M. Manos, J. Appl. Phys. **80**, 2643 (1996).
[16]T. Tsuchizawa, Y. Jin, and S. Matsuo, Jpn. J. Appl. Phys., Part 1 **33**, 2200 (1994).
[17]X. Tang, Q. Wang, and D. M. Manos, J. Vac. Sci. Technol. B **18**, 1262 (2000).
[18]N. Lorente, D. Teillet-Billy, and J. P. Gauyacq, Nucl. Instrum. Methods Phys. Res. B **157**, 1 (1999).
[19]J. F. Ziegler, J. P. Biersack, and U. Littmark, *The Stopping and Range of Ions in Solids* (Pergamon, New York, 1985).
[20]W. Eckstein and J. P. Biersack, Appl. Phys. A: Solids Surf. **A38**, 123 (1985).
[21]Y. Tokunaga, Y. Kurita, M. Sugihara, S. Hitoki, and S. Saito, Comput. Phys. Commun. **38**, 15 (1985).
[22]B. A. Helmer and D. B. Graves, J. Vac. Sci. Technol. A **16**, 3502 (1998).
[23]C. F. Abrams and D. B. Graves, J. Vac. Sci. Technol. A **16**, 3006 (1998).
[24]J. Reece Roth, *Industrial Plasma Engineering* (Institute of Physics, Bristol, UK, 1995), Vol. 1.